Second Harmonic Generation of C₆₀ Incorporated in Alkali Metal Ion Zeolites and Mesoporous MCM-41 Silica

José Raul Herance,[†,‡] Encarna Peris,[†] José Vidal,[§] José Luis Bourdelande,*[,‡] Jordi Marquet,[‡] and Hermenegildo García*[,†]

Instituto de Tecnología Química CSIC-UPV, Universidad Politécnica de Valencia, Avda de los Naranjos s/n, 46022 Valencia, Spain, Universitat Autònoma de Barcelona, Facultat de Ciències, Química Orgànica, Cerdanyola del Vallés, Barcelona, Spain, and Institut de Ciència de Materials de Barcelona (CSIC), Campus Universitat Autònoma de Barcelona, Cerdanyola del Vallès 08193, Barcelona, Spain

Different loadings of C₆₀ have been incorporated in mesoporous MCM-41 aluminosilicate as well as proton and alkali metal ion zeolites. These samples show non-linear optics activity whose efficiency increases upon C₆₀ content, size of the alkali metal ion, and laser exposure. The later unprecedented second harmonic generation (SHG) enhancement effect can lead up to 2 orders of magnitude efficiency increase. After having irradiated the solid, the SHG enhancement decays upon standing in the dark toward the initial value of fresh and unexposed samples. EPR measurements and alternative generation of zeolite electron−holes ions pairs have ruled out triplet excited states and radical ions as responsible for this enhancement upon irradiation. One proposal at the moment is that this SHG activity enhancement arises from unstable photoproducts such as photoadduct or dimers. However, attempts to isolate any C₆₀-derived photoproduct have met with failure so far.

Introduction

The ability of zeolites to host inside their internal voids organic guests can serve to prepare advanced materials in which the intrinsic molecular properties of the organic guest are controlled by immobilization and compartmentalization inside the rigid zeolite framework.[1−8] The geometry and topology of the zeolite micropores can be used to organize spatially the organic guest, while at the same time provides site isolation and stabilization of the guests by impeding the attack of atmospheric reagents.[9−12]

Second harmonic generation (SHG) is one of the properties in which the molecular response of the guest can be strongly influenced by incorporation inside the zeolite framework.[13−16] Among the best studied examples, one paradigmatic case is

p-nitroaniline, which is a molecule with a large dipole moment that could serve in principle for nonlinear optics.[9,17−20] However the fact that the most common *p*-nitroaniline crystal phase is centrosymmetric severely limits its use for SHG. In this case, the intensive work of Marlow and co-workers have shown that, upon inclusion of *p*-nitroaniline in the channels of zeolites and related ALPO₄-5 materials, the head-to-tail ordering inside the micropores makes a host−guest material that exhibits non-linear optics activity.[13,17,18,20] Hemicyanine exchanged inside ZSM-5 zeolite and (dimethylamino)benzonitrile in ALPO₄-5 constitute other examples of materials whose SHG activity increases upon incorporation inside zeolite particles.[21,22]

Despite its molecular symmetry, it is known that films of C₆₀ exhibit SHG activity arising from magnetic dipoles and electrical quadrupoles within the crystals.[23−28] Herein, we

* Corresponding author e-mail: hgarcia@qim.upv.es (H.G.); joseluis.bourdelande@uab.es (J.L.B.).
† Universidad Politécnica de Valencia.
‡ Universitat Autónoma de Barcelona.
§ Campus Universitat Autónoma de Barcelona.

(1) Garcia, H.; Roth, H. D. *Chem. Rev.* **2002**, *102*, 3947−4008.
(2) Scaiano, J. C.; García, H. *Acc. Chem. Res.* **1999**, *32*, 783−793.
(3) Vaidyalingam, A. S.; Coutant, M. A.; Dutta, P. K. *Electron Transfer Chem.* **2001**, *4*, 412−486.
(4) Dutta, P. K. *J. Inclusion Phenom. Mol. Recognit. Chem.* **1995**, *21*, 215−37.
(5) Bruhwiler, D.; Calzaferri, G. *Microporous Mesoporous Mater.* **2004**, *72*, 1−23.
(6) Corma, A.; Garcia, H. *Eur. J. Inorg. Chem.* **2004**, 1143−1164.
(7) Hashimoto, S. *J. Photochem. Photobiol. C* **2003**, *4*, 19−49.
(8) De Vos, D. E.; Jacobs, P. A. *Stud. Surf. Sci. Catal.* **2001**, *137*, 957−985.
(9) Herance, J. R.; Das, D.; Marquet, J.; Bourdelande, J. L.; Garcia, H. *Chem. Phys. Lett.* **2004**, *395*, 186−189.
(10) Herance, J. R.; Marquet, J.; Bourdelande, J. L.; Garcia, H. *Chem. Phys. Lett.* **2004**, *395*, 49−52.
(11) Calzaferri, G. *Chimia* **1998**, *52*, 525−532.
(12) Moller, K.; Bein, T. *Chem. Mater.* **1998**, *10*, 2950−2963.
(13) Caro, J.; Marlow, F.; Wuebbenhorst, M. *Adv. Mater.* **1994**, *6*, 413−16.
(14) Hoffmann, K.; Marlow, F. In *Handbook of Zeolite Science and Technology;* Auerbach, S. M., Carrado, K. A., Dutta, P. K., Eds.; Dekker: New York, 2003; pp 921−949.
(15) Marlow, F. *Mol. Cryst. Liq. Cryst. Sci. Technol. A* **2000**, *341*, 289−294.
(16) Schulz-Ekloff, G.; Wohrle, D.; van Duffel, B.; Schoonheydt, R. A. *Microporous Mesoporous Mater.* **2002**, *51*, 91−138.
(17) Gao, F.; Zhu, G.; Chen, Y.; Li, Y.; Qiu, S. *J. Phys. Chem. B* **2004**, *108*, 3426−3430.
(18) Kinski, I.; Daniels, P.; Deroche, C.; Marler, B.; Gies, H. *Microporous Mesoporous Mater.* **2002**, *56*, 11−25.
(19) Marlow, F.; Kornatowski, J.; Reck, B.; Leike, I.; Hoffmann, K.; Caro, J. *Mol. Cryst. Liq. Cryst. Sci. Technol. A* **1996**, *276*, 295−304.
(20) Werner, L.; Caro, J.; Finger, G.; Kornatowski, J. *Zeolites* **1992**, *12*, 658−63.
(21) Kim, H. S.; Lee, S. M.; Ha, K.; Jung, C.; Lee, Y.-J.; Chun, Y. S.; Kim, D.; Rhee, B. K.; Yoon, K. B. *J. Am. Chem. Soc.* **2004**, *126*, 673−682.
(22) Marlow, F.; Caro, J.; Werner, L.; Kornatowski, J.; Daehne, S. *J. Phys. Chem.* **1993**, *97*, 11286−90.
(23) Janner, A. M.; Jonkman, H. T.; Sawatzky, G. A. *Phys. Rev. B* **2001**, *63*, 085111/1−085111/6.

4098   *Chem. Mater., Vol. 17, No. 16, 2005*

Herance et al.

have prepared a series of powders containing C_{60} adsorbed inside the pores of zeolites and MCM-41 aluminosilicates and observed an enhanced SHG activity as a result of C_{60} encapsulation. The relative SHG efficiency has been found to depend on the structure and composition of porous host. Also an unprecedented gradual enhancement of the SHG efficiency as result of laser excitation has been observed.

Experimental Section

C_{60}-fullerene (Aldrich) and NaY (P. Q. Industries) were commercial samples and used as received. KY and CsY were obtained starting from NaY by submitting samples of this zeolite to alkali metal ion exchange at 50 °C using aqueous solutions of KAcO and CsAcO. The solid−liquid ratio of the ion exchanges was 1 to 10, and the suspensions were stirred magnetically for 6 h. To obtain the highest possible ion exchange level, two consecutive ion exchanges using 0.4 and 0.6 M solutions of K^+ or Cs^+ were carried out. Chemical analyses indicate that the Na^+ exchange was 85 and 70% for KY and CsY, respectively. $H\beta$ was obtained by air calcination at 550 °C of an as-synthesized β zeolite prepared by hydrothermal crystallization under continuous stirring at autogenous pressure and 150 °C using tetrapropylammonium bromide as structure directing agent, as previously reported.[29] MCM-41 was obtained by crystallization at 110 °C under static conditions and autogenous pressure for 4 days of clear gels of tetraethyl orthosilicate and aluminate using cetyltrimethylammonium as structure directing agent, as reported in the literature.[30,31] The structure of the aluminosilicate hosts was confirmed by powder X-ray diffraction, and surface area and pore volumes were measured by isothermal N_2 gas adsorption.

Adsorption of C_{60} onto the porous hosts was carried out by heating a mechanical mixture of C_{60} (50 mg) and NaY or $H\beta$ zeolite (1 g), C_{60} (10 mg), and CsY or KY zeolite (1 g), and C_{60} (10, 20, 40 mg) and MCM-41 (1 g) in a vacuum to 450 °C for 4 days. The samples were thoroughly extracted in Soxhlet using toluene as solvent to remove the non-incorporated C_{60}. The final C_{60} loading of toluene-free host−guest samples was determined by combustion chemical analyses using a Fisons CHNOS analyzer. Diffuse reflectance UV−Vis spectra were recorded in a Cary 5 G spectrophotometer adapted with an integrating sphere using $BaSO_4$ as reference. EPR spectra were recorded on a Bruker ER200D spectrometer working at X band (9.65 GHz) using DPPH ($g = 2.0036$) as reference.

SHG activity was measured for a 1064 nm YAG laser using the setup shown in Scheme 1. The powders were placed in a $2 \times 8 \times 40$ cm^2 quartz cuvette capped with a septum and purged with N_2 for at least 15 min before measurements. Urea powders or

Scheme 1. Setup Used for Determination of the Relative SHG Efficiency of Host−Guest Samples Containing C_{60}[a]
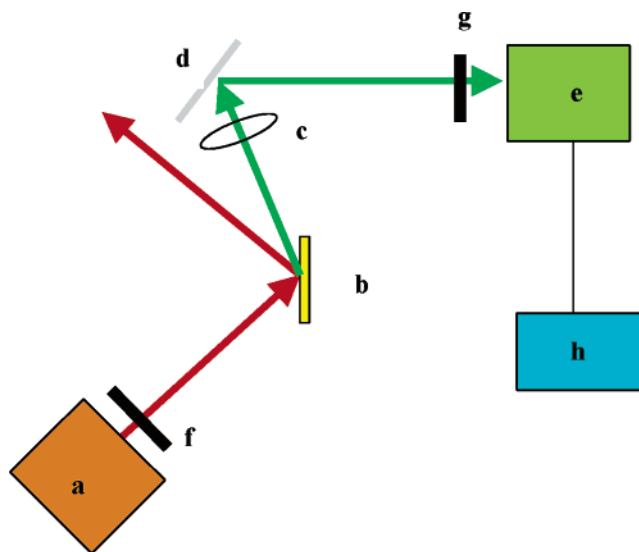
[a] Key: a, Nd:YAG laser operating at 1064 nm; b, sample cell; c, focusing lens; d, mirror; e, monochromator and photomultiplier; f and g, light filters; h, oscilloscope.

p-nitroaniline films were used as reference. Films of *p*-nitroaniline were obtained by depositing an ethanolic solution (100 μL) of *p*-nitroaniline (2.5 mg) on a quartz glass. Blank controls showed no significant SHG of zeolites or MCM-41. The power of the 532 nm signal measured for the blanks was below 0.1 mJ $\times$ $pulse^{-1}$.

Results and Discussion

Two types of materials in where C_{60} was included in the internal voids of either microporous zeolites or mesoporous MCM-41 silica were prepared. In the latter case, the large pore diameter of the MCM-41 (32 Å) as compared to C_{60} molecular size (crystallographic diameter 7.6 Å approximately)[32−34] makes adsorption much easier than in the case of microporous faujasites (7.4 Å pore size) or zeolite β (7.2 Å approximately).[35]

Due to the much easier adsorption,[36−39] samples of C_{60} incorporated in MCM-41 were used to explore the influence of guest loading on the relative SHG efficiency. Using MCM-41 as host, the loading of C_{60} can be more easily controlled varying the C_{60}−MCM-41 weight ratio during the adsorption process since most of the C_{60} becomes adsorbed on MCM-41 at a loading below 50 mg $\times$ g^{-1}, even after exhaustive washings to remove the externally adsorbed C_{60}. Nevertheless, it is obvious that an exact amount of incorporated C_{60}

(24) Mishina, E. D.; Fedyanin, A. A.; Klimkin, D.; Nikulin, A. A.; Aktsipetrov, O. A.; Vorob'eva, S. L.; Novak, V. R.; Devillers, M. A. C.; Rasing, T. *Surf. Sci.* **1997**, *382*, L696−L699.

(25) Hoshi, H.; Yamada, T.; Ishikawa, K.; Takezoe, H.; Fukuda, A. *Phys. Rev. B* **1995**, *52*, 12355−65.

(26) Zhang, T. G.; Xu, Z. Y.; Lundquist, P. M.; Lin, W. P.; Ketterson, J. B.; Wong, G. K.; Wang, X. K.; Chang, R. P. H. *Opt. Commun.* **1994**, *111*, 517−20.

(27) Koopmans, B.; Janner, A. M.; Jonkman, H. T.; Sawatzky, G. A.; van der Woude, F. *Phys. Rev. Lett.* **1993**, *71*, 3569−72.

(28) Qin, S.; You, W.; Su, Z. *Phys. Rev. B* **1993**, *48*, 17562−8.

(29) Camblor, M. A.; Mifsud, A.; Pérez-Pariente, J. *Zeolites* **1991**, *11*, 792−797.

(30) Kresge, C. T.; Leonowicz, M. E.; Roth, W. J.; Vartuli, J. C.; Beck, J. S. *Nature* **1992**, *359*, 710−712.

(31) Beck, J. S.; Vartuli, J. C.; Roth, W. J.; Leonowicz, M. E.; Kresge, C. T.; Schmitt, K. D.; Chu, C. T.-W.; Olson, D. H.; Sheppard, E. W.; McCullen, S. B.; Higgins, J. B.; Schlenker, J. L. *J. Am. Chem. Soc.* **1992**, *114*, 10834−10843.

(32) Sastre, G.; Cano, M. L.; Corma, A.; Garcia, H.; Nicolopoulos, S.; Gonzalez-Calbet, J. M.; Vallet-Regi, M. *J. Phys. Chem. B* **1997**, *101*, 10184−10190.

(33) Liu, S.; Lu, Y. J.; Kappes, M. M.; Ibers, J. A. *Science* **1991**, *254*, 408−10.

(34) Galletero, M. S.; Garcia, H.; Bourdelande, J. L. *Chem. Phys. Lett.* **2003**, *370*, 829−833.

(35) Meier, W. M.; Olson, D. H.; Baerlocher, C. *Zeolites* **1996**, *17*, 1−229.

(36) Rachdi, F.; Hajii, L.; Goze, C.; Jones, D. J.; Mairles-Torres, P.; Roziere, J. *Solid State Commun.* **1996**, *100*, 237−240.

(37) Gu, G.; Ding, W.; Du, Y.; Huang, H.; Yang, S. *Appl. Phys. Lett.* **1997**, *70*, 2619−2621.

(38) Lee, C.-H.; Lin, T.-S.; Lin, H.-P.; Zhao, Q.; Liu, S.-B.; Mou, C.-Y. *Microporous Mesoporous Mater.* **2003**, *57*, 199−209.

(39) Govindaraj, A.; Nath, M.; Eswaramoorthy, M. *Chem. Phys. Lett.* **2000**, *317*, 35−39.

Table 1. List of the Host−Guest Samples Studied in This Work and the Main Textural, Porosity, and Analytical Data

sample name	host	particle size (μm)	pore diameter (Å)	surface area ($m^2 \times g^{-1}$)	C_{60} content (% C)
C_{60}−Hβ	β	0.1	windows: 7.2 elliptical cavities: 11 × 7.2	550	2.65
C_{60}−NaY	Y	1	windows: 7.4 spherical cavities: 12.5 diameter	654	1.30
C_{60}−KY					0.12
C_{60}−CsY					0.12
C_{60}−MCM-41	MCM-41	0.1−0.3	channels: 32	874	0.61
					0.87
					2.43

on MCM-41 after adsorption and washings is not controllable, and combustion chemical analysis is necessary to determine the loading.

In the case of microporous zeolites, incorporation inside the micropores is more problematic and less easily controllable due to the fact that the pore size is smaller than the C_{60} diameter. For this reason, incorporation of C_{60} inside zeolites requires prolonged thermal treatment at high temperatures in evacuated cells.[32,34,40−42] High adsorption temperature favors framework vibrational motion reaching instantaneous pore dimensions larger than the C_{60} crystallographic diameter. In addition, high temperature increases the kinetic energy of the diffusing molecules favoring their penetration inside the pores. Theoretical calculations confirmed by experimental characterization have shown that inclusion of C_{60} in the cavities of tridirectional large pores zeolite becomes possible at high temperatures.[32]

For our study, we have included C_{60} in a series of alkali metal ion exchanged Y zeolites. The nature of the alkali metal ion should influence the electronic density on the adsorbed C_{60} through charge-transfer zeolite framework−C_{60} complex formation, the zeolite framework oxygens acting as electron donors and the incorporated C_{60} as electron acceptor. In this regard, it is well-established that the electron density of zeolite framework oxygen, and therefore the electron donor ability of the zeolite, increases in the series $Na^+ < K^+ < Cs^+$.[43−48] Also the influence of the alkali metal ion modulating the strength of the charge-transfer complexes between the zeolite framework and organic guests has been previously demonstrated.[44,48,49] In our study we also included samples of C_{60} adsorbed in zeolite β. The list of materials prepared, the C_{60} content and some relevant textural and porosity data are summarized in Table 1.

All the samples containing C_{60} exhibit activity for SHG. The experimental setup used to determine the relative SHG efficiency of the samples under study is depicted in Scheme 1. The most relevant feature of our setup is that the exposed surface of the powder placed in a 2 × 8 × 40 mm quartz cell is excited with a 1064 nm laser pulse at 45° and the scattered light collected in a angle to 10°−40°. The scattered

Table 2. Results of the Relative SHG Efficiency of C_{60}−MCM-41 Samples Differing on the C_{60} Loading Measured after 1 or 90 Laser Pulses[a]

C_{60}−MCM-41 loading (% C)	efficiency in first pulse (arbitrary units)	efficiency after 90 pulses (arbitrary units)
0.61	379	7577
0.87	399	9177
2.43	259	3846

[a] A film of *p*-nitroaniline under the same conditions gave a SHG efficiency of 180 detector counts.

light is filtered with a 532 nm interference filter and focused onto a monochromator set at 532 nm before reaching the photomultiplier tube. Measurements of the relative efficiency were done for the samples under study in order to determine the influence of C_{60} loading, the solid host, and the nature of the charge balancing cation. As standard samples with respect to which compare the SHG efficiency of the zeolite encapsulated C_{60}, we have used films of *p*-nitroaniline and urea crystals.

As expected, the relative efficiency for SHG in the series of C_{60} incorporated in MCM-41 is influenced by the loading of C_{60}. With the set of three C_{60}−MCM-41 samples prepared, the maximum SHG efficiency was observed for the 0.87 wt %, C_{60}−MCM-41 samples with lower or higher loadings leading to a decrease in the SHG efficiency. The lack of a linear relationship between SHG activity and C_{60} loading indicates the occurrence of re-absorption and saturation phenomenona. The actual values of SHG efficiency are listed in Table 2. Control experiments in where pristine MCM-41 was submitted to the same study showed negligible SHG activity of the porous silicate host as compared to C_{60}−MCM-41.

In addition to C_{60} loading, the SHG also depended on the structure of the host. Changing from mesoporous MCM-41 to microporous zeolites produces a significant increase on the efficiency that is even more remarkable when specific values (i.e., the relative efficiency per gram of incorporated C_{60}) are compared. This may reflect the site isolation experienced by C_{60} inside a zeolite cage as well as specific host−guest interactions arising from the closer contact between the C_{60} and the silicate framework. Thus, the channel structure of MCM-41 should not produce site isolation, and lateral contact between adsorbed C_{60} molecules should be still possible in MCM-41 but not in zeolites. On the other hand the internal surface of MCM-41 contains a high population of silanol groups (about 30% of the total Si atoms) while the population of silanols in faujasites is negligible.

In this regard, it is very informative the trend observed for SHG efficiency as a function of the nature of the alkali metal ion. The measurements of relative efficiencies are listed

(40) Kwon, O. H.; Yoo, H.; Jang, D. J. *Eur. Phys. J. D* **2002**, *18*, 69−75.
(41) Kwon, O.-H. *J. Phys. Chem. B* **2001**, *105*, 4195−4199.
(42) Jeon, I. C.; Hong, S. B. *Bull. Korean Chem. Soc.* **1993**, *14*, 305−7.
(43) Barthomeuf, D. *Microporous Mesoporous Mater.* **2003**, *66*, 1−14.
(44) Hashimoto, S. *Tetrahedron* **2000**, *56*, 6957−6963.
(45) Barthoomeuf, D. *Catal. Rev.* **1996**, *38*, 521−612.
(46) Huang, M.; Kaliaguine, S.; Auroux, A. *Stud. Surf. Sci. Catal.* **1995**, *97*, 311−18.
(47) Barthomeuf, D. *NATO ASI Ser. C* **1994**, *444*, 181−97.
(48) Alvaro, M.; García, H.; García, S.; Márquez, F.; Scaiano, J. C. *J. Phys. Chem.* **1997**, *101*, 3043−3051.
(49) Park, Y. S.; Um, S. Y.; Yoon, K. B. *J. Am. Chem. Soc.* **1999**, *121*, 3193−3200.

4100 *Chem. Mater., Vol. 17, No. 16, 2005*

Herance et al.

Table 3. Measurements of the Relative SHG Efficiency for the Zeolite Containing C_{60} as a Function of the Number of 1064 nm Laser Pulses to Which the Surface Was Exposed[a]

no. of laser pulses	efficiency $C_{60}-H\beta$ (arbitrary units)	efficiency $C_{60}-NaY$ (arbitrary units)	efficiency $C_{60}-KY$ (arbitrary units)	efficiency $C_{60}-CsY$ (arbitrary units)
1	619	367	22054	26089
10	699	1719	31402	26736
90	1730	8129	43532	41918

[a] A film of *p*-nitroaniline under the same conditions gave a SHG efficiency of 180 detector counts.
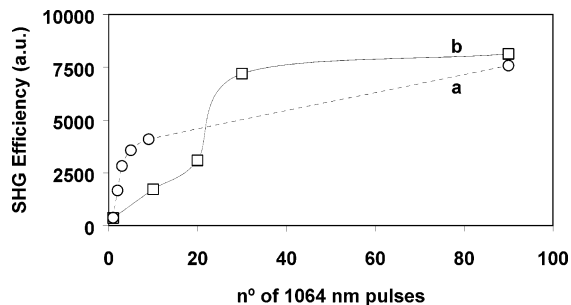

Figure 1. Plot of the variation of the relative SHG efficiency for $C_{60}-$MCM-41 at 0.87% loading (a) and $C_{60}-NaY$ (b) as a function of the number of laser pulses to which the solid sample is exposed.

in Table 3. We have observed that the more basic the zeolite framework, the higher SHG efficiency. It is well-known that the basicity of framework and the electron density of the framework oxygens increase along the radius of the alkali metal ion.[43,47,50] This higher electron density of the zeolite oxygen will favor the interaction with C_{60} most probably by formation of a charge-transfer zeolite C_{60} complex. This type of charge-transfer complexes where separately alkali-metal exchanged faujasites act as electron donor against an electron acceptor[44,48,49] and, on the other hand, C_{60} acts as electron acceptor against electron donor couples are well documented.[51-54] Here our claim is that a charge-transfer complex leading to an enhancement of the SHG efficiency is established between electron-rich, basic zeolite frameworks and adsorbed C_{60} guests. Whatever the reason responsible for the influence of the zeolite composition on the SHG efficiency, the data of Table 3 clearly show that the intrinsic activity for SHG of C_{60} can be modulated by interaction with the aluminosilicate host in a systematic and predictable manner.

As can be inferred from Tables 2 and 3, a general phenomenon observed for all the samples is a remarkable increase in the SHG efficiency with the number of laser pulses at which the samples were exposed until a plateau is reached at long exposures. Two extreme examples to illustrate the above point are shown in Figure 1, where the variation of the relative SHG efficiency as a function of the
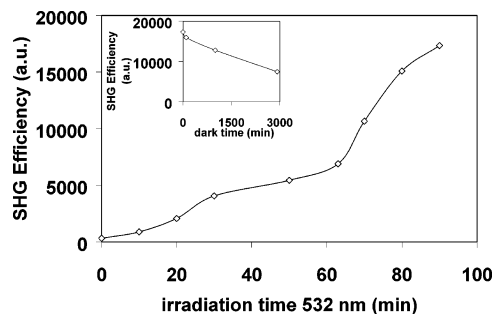
(50) Barthomeuf, D.; Coudurier, G.; Vedrine, J. C. *Mater. Chem. Phys.* **1988**, *18*, 553−75.
(51) Catalan, J.; Saiz, J. L.; Laynez, J. L.; Jagerovic, N.; Elguero, J. *Angew. Chem., Int. Ed. Engl.* **1995**, *34*, 105−7.
(52) Ivannikov, A. V.; Gun'kin, I. F. *Rus. J. Gen. Chem.* **2003**, *73*, 627−629.
(53) Konarev, D. V.; Shul'ga, Y. M.; Roshchupkina, O. S.; Lyubovskaya, R. N. *J. Phys. Chem. Solids* **1997**, *58*, 1869−1872.
(54) Llacay, J.; Tarres, J.; Rovira, C.; Veciana, J.; Mas, M.; Molins, E. *J. Phys. Chem. Solids* **1997**, *58*, 1675−1678.

Figure 2. Plot of the SHG efficiency of the $C_{60}-$MCM-41 sample (loading $0.87 \text{ g} \times \text{g}^{-1}$) as a function of the lamp irradiation time. Irradiation was performed with a 150 W xenon Arc lamp, and the light was filtered with a yellow subtractive filter (Andover 520FD22-50S) and a cyan subtractive filter (Andover 590FD24-50S). The inset shows the decay of the SHG efficiency of lamp-irradiated $C_{60}-$MCM-41 (0.87 C %) as a function of the time elapsed after irradiation.
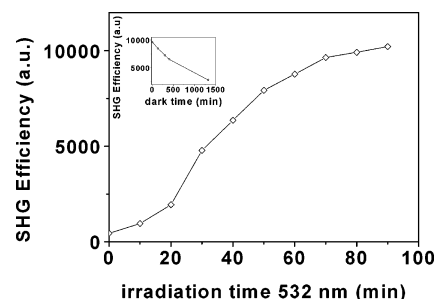

Figure 3. Plot of the SHG efficiency of the $C_{60}-NaY$ sample as a function of the time of irradiation with a 150 W xenon Arc lamp, and the light was filtered with a yellow subtractive filter (Andover 520FD22-50S) and a cyan subtractive filter (Andover 590FD24-50S). The insert shows the decay of the SHG efficiency of an irradiated sample upon storage in the dark for increasing time.
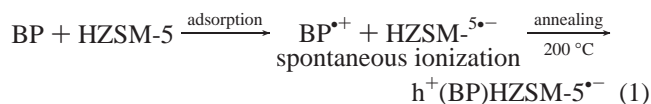
number of 1064 nm laser pulses to which the sample was exposed is presented. While the profile of SHG efficiency enhancement for some $C_{60}-$MCM-41 samples (see Figure 1 for the sample at 0.87% C_{60} loading) follows a single-exponential growth, suggesting that this effect is related to the population of unaltered C_{60}. The enhancement profile for C_{60} hosted in microporous zeolites (see profile for $C_{60}-$NaY in Figure 1) exhibits a sigmoid shape that could be related to an induction or pre-activation process.

Noteworthy, in some cases up to 2 orders of magnitude increase in the relative value of SHG efficiency was observed. To explain this phenomenon, we submitted samples to lamp irradiation with visible light (520 nm < λ < 580 nm) for a certain time and compared the efficiency of the fresh and irradiated samples as a function of the exposure time. The lamp-irradiated zeolites containing C_{60} exhibited always higher SHG efficiency than the same sample stored in the dark (Figures 2 and 3), thus indicating that a photochemically generated species is responsible for the SHG enhancement. Control experiments using pristine zeolites showed, as in the cases of MCM-41, a very weak response that even decreases to negligible values with the number of laser pulses. When the irradiated sample, irrespective of whether irradiation was by laser flash or by continuous lamp, was left in the dark for long periods, there was a gradual and continuous decay of the SHG efficiency within hours until after 2 days values very close (but still higher) to the activity of the corresponding fresh samples were again measured.

This SGH activity enhancement can be rationalized assuming that during the SHG experiments reabsorption of the 532 nm radiation by C_{60} takes place. C_{60} in its excited triplet electronic states would form an unstable photochemical product that has a significantly higher efficiency for SHG than C_{60}. To determine the nature of this photochemically generated intermediate, EPR measurements were carried out. As expected in view of the precedents in the literature,[55-57] EPR spectroscopy reveals the presence of C_{60} radical cation in all the samples of porous silicate containing C_{60} as assessed by the observation of a signal at $g = 2.0022$ that agrees relatively well with the g value of 2.0027 ± 0.0002 reported in the literature for the $C_{60}^{\bullet+}$ incorporated in FeY zeolite.[58,59] This g value is significantly different to the g value of $C_{60}^{\bullet-}$ that appears at $g = 2.0000$; therefore, the radical anion that is the C_{60} transient species more frequently observed in solution can be firmly ruled out in our case.[55] It has to be noted that although EPR detects $C_{60}^{\bullet+}$, this has to be a minor species since diffuse reflectance UV−Vis spectroscopy is not able to detect its presence and only neutral C_{60} molecules can be observed by steady-state optical spectroscopy. In this regard the bias of EPR to detect organic radical cation due to its extreme sensitivity is well-known.[1] Upon irradiation of these samples, the signal of $C_{60}^{\bullet+}$ even weakens, and a broad band appears under these conditions.

Considering the recent work of Bremard, Moisette et al. that have shown the formation of electron and holes in the zeolite during the aging of organic radical cations,[60-63] we also explored the possibility that these electron−hole pairs generated from $C_{60}^{\bullet+}$ could be somehow responsible for the increase in the non linear optics response of the porous aluminosilicate samples. These species derived from $C_{60}^{\bullet+}$ radical cation would be associated with the broad EPR band recorded in our samples. To address this possibility, we prepared a series of zeolite samples containing electron and holes by adsorbing increasing amounts of biphenyl (BP) in a protonic ZSM-5 and after observing $BP^{\bullet+}$ generation by diffuse reflectance UV−Vis spectroscopy, the sample was annealed at 200 °C to form zeolite holes as reported.[60,61] Equation 1 describes the alternative strategy followed for the generation of electron and holes in the absence of C_{60}. When these samples derived from BP were scrutinized for their SHG efficiency, the response was very weak (< 10% of the response of fresh C_{60}) and even decreased upon laser exposure (Table 4), just the opposite behavior observed for C_{60} incorporated in micro- and mesoporous aluminosilicates:

$$BP + HZSM\text{-}5 \xrightarrow[\text{spontaneous ionization}]{\text{adsorption}} BP^{\bullet+} + HZSM\text{-}5^{\bullet-} \xrightarrow[200\ °C]{\text{annealing}}$$
$$h^+(BP)HZSM\text{-}5^{\bullet-} \quad (1)$$

Thus, considering all the available data (i.e., low population of $C_{60}^{\bullet+}$ radical cations not detectable by optical

Table 4. Measurements of the Relative SHG Efficiency of a Series of BP−HZSM-5 Samples Containing Increasing Amounts of BP as a Function of the Number of 1064 nm Laser Shots[a]

	SHG efficiency	
% C	1 pulse (arbitrary units)	8 pulses (arbitrary units)
0.174	7741	1816
0.206	6539	1534
0.368	3660	859
1.011	1332	313
1.269	1061	249
2.241	601	141

[a] BP−HZSM-5 samples were annealed as indicated in eq 1 to generate variable amounts of electrons and holes. Under the same circumstances, a film of *p*-nitroaniline gives 1550 detector counts.

spectroscopy, no participation of zeolite electrons and holes, lifetime of the decay of enhanced signal toward initial values in tens of hours, and photochemical origin of the effect), the most reasonable explanation for the dramatic enhancement of SHG efficiency is the formation of an unstable photochemical product, photoadducts or dimeric products being the most likely species at this moment in view of the well-known photochemistry of C_{60}.[64-66] The induction period observed in the profile of SHG efficiency increase upon photochemical irradiation seems to indicate the formation of an intermediate or/and relocation of C_{60} previous to the efficiency enhancement effect.

We notice, however, that to determine the nature of the photogenerated species responsible of the SHG enhancement effect inside zeolites is a very problematic task given the low guest loading and the need to attack the zeolite framework with concentrated hydrofluoric acid. On top of that, it is particularly difficult in this case in where the photoproduct appears to decay over the time.

Nevertheless, aiming to gain some information about the nature of the photoproduct, some additional experiments were carried out. Upon exhaustive Ar purge, the same SHG enhancement effect is observed. Although Ar purging does not rule out the complete absence of O_2, the observation of the same behavior under Ar and under air suggests the lack of participation of O_2 on this phenomenon. It is well demonstrated, on the other hand, that O_2 diffusion on hydrated hydrophilic zeolites is very problematic or does not occur since the micropore voids are almost completely filled with water.[2] On the other hand, dimers and oligomers cannot fit inside the faujasites supercages. Thus, in case that these photoadducts were responsible for the photochemical SHG enhancement, these photoadducts could only be formed on the external surface of the particles, at defect sites, or through

(55) Kukolich, S. G.; Huffman, D. R. *Chem. Phys. Lett.* **1991**, *182*, 263−5.
(56) Yang, C. C.; Hwang, K. C. *J. Am. Chem. Soc.* **1996**, *118*, 4693−8.
(57) Stankowski, J.; Martinek, J.; Koper, A.; Kempinski, W. *Mol. Phys. Rep.* **1994**, *5*, 33−9.
(58) Fukuzumi, S.; Suenobu, T.; Urano, T.; Tanaka, K. *Chem. Lett.* **1997**, 875−876.
(59) Keizer, P. N.; Morton, J. R.; Preston, K. F.; Sugden, A. K. *J. Phys. Chem.* **1991**, *95*, 7117−18.
(60) Moissette, A.; Vezin, H.; Gener, I.; Patarin, J.; Bremard, C. *Angew. Chem., Int. Ed.* **2002**, *41*, 1241−1244.
(61) Vezin, H.; Moissette, A.; Bremard, C. *Angew. Chem., Int. Ed.* **2003**, *42*, 5587−5591.
(62) Moissette, A.; Vezin, H.; Gener, I.; Bremard, C. *J. Phys. Chem. B* **2003**, *107*, 8935−8945.
(63) Moissette, A.; Marquis, S.; Gener, I.; Bremard, C. *Phys. Chem. Chem. Phys.* **2002**, *4*, 5690−5696.
(64) Akselrod, L.; Byrne, H. J.; Thomsen, C.; Roth, S. *Mol. Cryst. Liq. Cryst. Sci. Technol. A* **1994**, *256*, 833−8.
(65) Akselrod, L.; Byrne, H. J.; Thomsen, C.; Roth, S. *Chem. Phys. Lett.* **1993**, *215*, 131−6.
(66) Tsyboulski, D.; Heymann, D.; Bachilo, S. M.; Alemany, L. B.; Weisman, R. B. *J. Am. Chem. Soc.* **2004**, *126*, 7350−7358.

the cavity windows. Therefore only a low population of the total included C_{60} guest could participate in the process. It is worth commenting on, however, a recent report showing that photodimers of $C_{60}O$ formed in high yields revert to the corresponding monomer.[66] Also it should be mentioned that all our attempts to isolate a C_{60}-derived photoproduct from irradiated C_{60} hosted in zeolites were unsuccessful, the only compound detected being unaltered C_{60}. Whatever the nature of the photoproducts responsible for the SHG enhancement, what is remarkable is that this effect is not observed in other media. Particularly, the SHG ability of C_{60} in polystyrene films has also been studied, and it was found that this material undergoes bleaching and SHG efficiency decrease along the laser exposure.[67−71] This is in contrast to the increase on SHG efficiency observed for C_{60}−zeolite samples.

In summary, in the present work we have reported the observation of SHG effect for C_{60} samples embedded in meso- and microporous silicates. The SHG depend clearly on the nature of the host as well as on the nature of the alkali metal ion accompanying to C_{60}. An unprecedented 2 orders of magnitude enhancement of the SHG efficiency has been observed for all samples upon irradiation. This effect eventually diminishes within the time scale of days toward the initial values of fresh, unexposed samples. Although the exact nature of the photochemically generated species is uncertain at the moment, the present data rules out the involvement of triplet excited states, radical ions, and zeolite electron and hole pairs, the most reasonable species responsible for this effect being unstable photoadducts located at the external surface. As far as we know, this observation of SHG efficiency enhancement is specific of incorporation of C_{60} inside aluminosilicate porous hosts and contrasts with self-degradation and bleaching reported for C_{60}-polystyrene films.

(67) Sun, Y.-P.; Riggs, J. E. *J. Chem. Soc., Faraday Trans.* **1997**, *93*, 1965−1970.
(68) Venturini, J.; Koudoumas, E.; Couris, S.; Janot, J. M.; Seta, P.; Mathis, C.; Leach, S. *J. Mater. Chem.* **2002**, *12*, 2071−2076.
(69) Couris, S.; Konstantaki, M.; Koudoumas, E.; Ederle, Y.; Mathis, C.; Leach, S.; Seta, P. *Mol. Cryst. Liq. Cryst. Sci. Technol. B* **2001**, *27*, 269−277.
(70) Koudoumas, E.; Konstantaki, M.; Mavromanolakis, A.; Couris, S.; Ederle, Y.; Mathis, C.; Seta, P.; Leach, S. *Chem. Phys. Lett.* **2001**, *335*, 533−538.
(71) Bourdelande, J. L.; Font, J.; Gonzalez-Moreno, R. *Helv. Chim. Acta* **2001**, *84*, 3488−3494.